



저작자표시 2.0 대한민국

이용자는 아래의 조건을 따르는 경우에 한하여 자유롭게

- 이 저작물을 복제, 배포, 전송, 전시, 공연 및 방송할 수 있습니다.
- 이차적 저작물을 작성할 수 있습니다.
- 이 저작물을 영리 목적으로 이용할 수 있습니다.

다음과 같은 조건을 따라야 합니다:



저작자표시. 귀하는 원저작자를 표시하여야 합니다.

- 귀하는, 이 저작물의 재이용이나 배포의 경우, 이 저작물에 적용된 이용허락조건을 명확하게 나타내어야 합니다.
- 저작권자로부터 별도의 허가를 받으면 이러한 조건들은 적용되지 않습니다.

저작권법에 따른 이용자의 권리는 위의 내용에 의하여 영향을 받지 않습니다.

이것은 [이용허락규약\(Legal Code\)](#)을 이해하기 쉽게 요약한 것입니다.

[Disclaimer](#) 

공학석사학위논문

**Effect of Surface Characteristics of
Reduced Graphene Oxide
on the Performance of Pseudocapacitor**

환원된 그래핀 옥사이드의 표면특성이
유사커패시터 성능에 미치는 영향

2015년 1월

서울대학교 대학원

재료공학부

장 미 세

Abstract

Effect of Surface Characteristics of Reduced Graphene Oxide on the Performance of Pseudocapacitor

Chang, Mi Se

Department of Material Science and Engineering

The Graduate School

Seoul National University

It is well known that reduced graphene oxide (rGO) has been intensely researched for applications in supercapacitors and rGO/metal oxide composite have also been spotlighted for its pseudocapacitive effects. Though metal oxides have high specific capacitance and electrochemical stability, they also show poor rate capability and low accessible surface areas. In order to overcome these problems, many fabrication methods of the composite has been suggested, such as, microwave assisted reflux methods by Rao et al., and electrochemical deposition method by Cao et al., which showed high specific capacitance values. However, other than just fabricating a composite and showing that it has a high value as listed above, no research has been done on verifying which kind of rGO plays the ideal role as a substrate for metal oxide composites in terms of rGO's surface characteristics, chemical properties, and

preparation methods.

Therefore, it came to our interest, that in order to fabricate rGO/metal oxide supercapacitor with high electrochemical performance, not only do we need to research on the composite fabrication methods, but also need to provide a guideline of how to prepare rGO substrate of different size, and functional groups. In this research, we analyzed the electrochemical characteristics of the different rGO/Co₃O₄ composites prepared by controlling rGO's surface characteristics and its relationship between the performance of the pseudocapacitor, providing a guideline for the ideal fabrication of rGO/metal oxide composite for pseudocapacitor. This way, further researches using rGO as electrode material for pseudocapacitors can, from now on, take our research into account for improved electrochemical performances.

keywords: reduced graphene oxide, oxygen functional groups, metal oxide, electrochemical performance, pseudocapacitor.

Student Number : 2012-23927

Contents

Abstract.....	i
Contents	iii
List of Tables	vi
List of Figures	vii
1. Introduction.....	9
1.1 Introduction to rGO/Co ₃ O ₄ pseudocapacitor.....	9
1.1.1 rGO as electrode material for supercapacitor and its EDLC behavior	9
1.1.2 Metal oxide (MO) as electrode material for pseudocapacitor and its pseudocapacitive behavior	11
1.1.3 Important factors for performance of pseudocapacitor	13
1.1.4 State-of-the-art (SOA) of rGO/Co ₃ O ₄ pseudocapacitors ...	14
1.1.5 Limitation of the state-of-the-art of rGO/Co ₃ O ₄ pseudocapacitors	17
1.2 The growth of metal oxide on the oxygen functionalized rGO substrate	18
1.2.1 Interaction of rGO and metal oxides	18
1.2.2 Growth of metal oxides and its interaction with the functional groups of the rGO	19
1.2.3 Controlling the functional groups of rGO through oxidation	

.....	20
1.2.4 Graphite precursors	22
1.3 The goal of this research	23
2. Experimental.....	25
2.1 Preparation of varied surface properties of rGO	25
2.1.1 Materials	25
2.1.2 Oxidation of GO(C) and GO(P).....	25
2.1.3 Oxidation of GO(P) at 0h, 4h, 8h, 16h oxidation time	26
2.2 Preparation of rGO/Co ₃ O ₄ pseudocapacitor.....	26
2.2.1 Preparation of rGO/Co ₃ O ₄ composites	26
2.2.2 Preparation of rGO/Co ₃ O ₄ electrodes.....	27
2.3 Characterization of rGO/Co ₃ O ₄ pseudocapacitor	28
2.3.1 Electrochemical measurement for electrochemical performance of pseudocapacitor	28
2.3.2 Physicochemical analysis of pseudocapacitor	28
3. Results and Discussion.....	29
3.1 Electrochemical and physicochemical analysis of rGO/Co ₃ O ₄ (C) and rGO/Co ₃ O ₄ (P).....	29
3.1.1 Electrochemical performance and structural analysis of rGO and Co ₃ O ₄	29

3.1.2 Electrochemical performance of rGO/Co ₃ O ₄ (C) and rGO/Co ₃ O ₄ (P)	32
3.1.3 Physicochemical analysis of GO(C), GO(P), rGO/Co ₃ O ₄ (C), and rGO/Co ₃ O ₄ (P).....	35
3.2 Electrochemical and physicochemical analysis of rGO/Co ₃ O ₄ (P- 0), rGO/Co ₃ O ₄ (P-4), rGO/Co ₃ O ₄ (P-8), rGO/Co ₃ O ₄ (P-16).....	39
3.2.1 Physicochemical analysis of GO(P-0), GO(P-4), GO(P-8), GO(P-16) and rGO/Co ₃ O ₄ (P-0), rGO/Co ₃ O ₄ (P-4), rGO/Co ₃ O ₄ (P-8), rGO/Co ₃ O ₄ (P-16).....	39
3.2.2 Electrochemical analysis of rGO/Co ₃ O ₄ (P-0), rGO/Co ₃ O ₄ (P- 4), rGO/Co ₃ O ₄ (P-8), rGO/Co ₃ O ₄ (P-16)	46
3.3 Correlation graphs.....	49
4. Conclusion	51
5. Reference	52

List of Tables

Table 1: SOA of rGO/Co ₃ O ₄ pseudocapacitors.....	15
Table 2: Calculated specific capacitance values of rGO, Co ₃ O ₄ , rGO/Co ₃ O ₄ (P), and rGO/Co ₃ O ₄ (C) at 1 Ag ⁻¹	33
Table 3: Amount of oxygenated carbon calculated from the XPS data of GO(P) and GO(C).....	37
Table 4: Percentages of oxygenated carbon calculated from the XPS data of GO(P-0), GO(P-4), GO(P-8), GO(P-16)	40
Table 5: Particle sizes and surface coverage of Co ₃ O ₄ grown on rGO/Co ₃ O ₄ (P- 0), rGO/Co ₃ O ₄ (P-4), rGO/Co ₃ O ₄ (P-8), rGO/Co ₃ O ₄ (P-16)	45
Table 6: Calculated specific capacitance values of rGO/Co ₃ O ₄ (P-0), rGO/Co ₃ O ₄ (P-4), rGO/Co ₃ O ₄ (P-8), rGO/Co ₃ O ₄ (P-16) at 1 Ag ⁻¹	48

List of Figures

Figure 1: Global Market for Graphene-based Products, 2009-2020 (\$ Millions)	10
Figure 2: a) Behavior of EDLC b) cyclic voltammetry of EDLC.....	11
Figure 3: a) Behavior of pseudocapacitor b) cyclic voltammetry of pseudocapacitor	12
Figure 4: a) Cyclic voltammetry of rGO/Co ₃ O ₄ pseudocapacitor with varying ratio b) Specific capacitances of rGO/Co ₃ O ₄ pseudocapacitor.....	16
Figure 5: Reaction scheme of reaction between MO and GO	18
Figure 6: SOA suggesting the difference in growth of MO depending on functional groups attached on GO	19
Figure 7: Steps of oxidation of GO	21
Figure 8: Expectation of the growth of MO on the varied functionalized GO surfaces	22
Figure 9: Optical microscopy images of a) small/crumpled GO and b) large/planar GO	23
Figure 10: Cyclic voltammetry of rGO	29
Figure 11: XRD of rGO	30
Figure 12: Cyclic voltammetry of Co ₃ O ₄	31
Figure 13: XRD of Co ₃ O ₄	31
Figure 14: Cyclic voltammetry of rGO/Co ₃ O ₄ (P), rGO/Co ₃ O ₄ (C), Co ₃ O ₄ , and rGO at 5 mV/s	33
Figure 15: XRD of Co ₃ O ₄ , rGO/Co ₃ O ₄ (P), rGO/Co ₃ O ₄ (C).....	35
Figure 16: Deconvoluted C1s peak of XPS data of a) GO(P) and b) GO(C)	36
Figure 17: SEM images of a) rGO/Co ₃ O ₄ (P) and b) rGO/Co ₃ O ₄ (C)	38

Figure 18: Deconvoluted C1s peak of XPS data of a) GO(P-0) and b) GO(P-4) c) GO(P-8) d) GO(P-16).....	40
Figure 19: XRD of Co_3O_4 , rGO/ Co_3O_4 (P-0), rGO/ Co_3O_4 (P-4), rGO/ Co_3O_4 (P-8), rGO/ Co_3O_4 (P-16).....	42
Figure 20: SEM images of a) rGO/ Co_3O_4 (P-0) b) rGO/ Co_3O_4 (P-4) c) rGO/ Co_3O_4 (P-8) d) rGO/ Co_3O_4 (P-16).....	43
Figure 21: TEM images of a) rGO/ Co_3O_4 (P-0) b) rGO/ Co_3O_4 (P-4) c) rGO/ Co_3O_4 (P-8) d) rGO/ Co_3O_4 (P-16).....	44
Figure 22: EDS measurements of rGO/ Co_3O_4 (P-16)	46
Figure 23: Cyclic voltammograms of rGO/ Co_3O_4 (P-0), rGO/ Co_3O_4 (P-4), rGO/ Co_3O_4 (P-8), rGO/ Co_3O_4 (P-16) at 5 mV/s	48
Figure 24: Correlation graphs of a) specific capacitance vs. samples rGO/ Co_3O_4 (P-0), rGO/ Co_3O_4 (P-4), rGO/ Co_3O_4 (P-8), rGO/ Co_3O_4 (P-16) at 1 A/g. b) specific capacitance vs. oxygen functional groups for rGO/ Co_3O_4 (P-0), rGO/ Co_3O_4 (P-4), rGO/ Co_3O_4 (P-8), rGO/ Co_3O_4 (P-16) at 1 A/g	50

1. Introduction

1.1 Introduction to rGO/Co₃O₄ pseudocapacitor

1.1.1 rGO as electrode material for supercapacitor and its EDLC behavior

Reduced graphene oxide (rGO), a 3-D stacked layers of oxygenated graphene, has been researched in many areas such as catalysts [1], hydrogen storage [2], organic solar cells [3], supercapacitors [4] and etc. As seen in Figure 1 [5], It has been statistically analyzed that graphene-based products will increase dramatically in less than 10 years, especially in the area of capacitors. Therefore, many researches have been done on using rGO as a substrate material for supercapacitor and are still in progress.

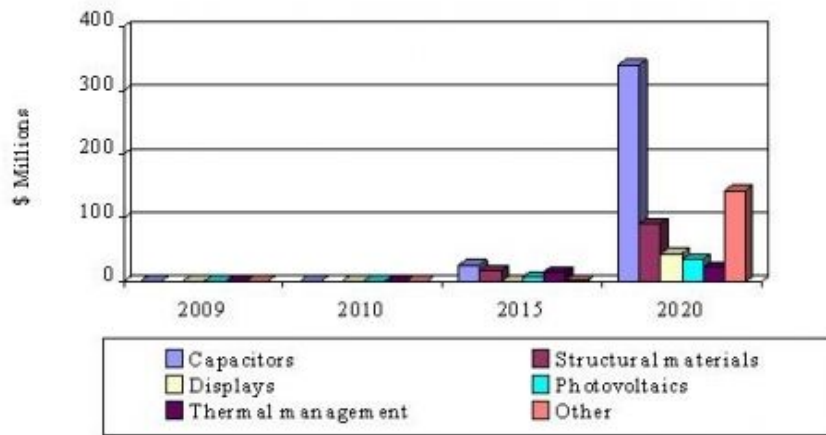


Figure 1: Global Market for Graphene-based Products, 2009-2020 (\$ Millions)

rGO has many advantages such as having wide potential window, large surface area, good flexibility, and good chemical & thermal stability [6]. Because of its large surface area, it is suitable to be used as a porous substrate for supercapacitor as porosity and surface area is an important factor when discussing the electrochemical performance of supercapacitors [7]. As shown in Figure 2a [8], rGO usually shows an electric double layer capacitance behavior (EDLC) because it interacts with electrolyte ions through electrostatic reactions where the ions solely adsorb onto the surface of the rGO substrate without chemical reaction [9]. Thus, providing a cyclic voltammetry graph of a symmetrical and rectangular shape as seen in Figure 2b [8].

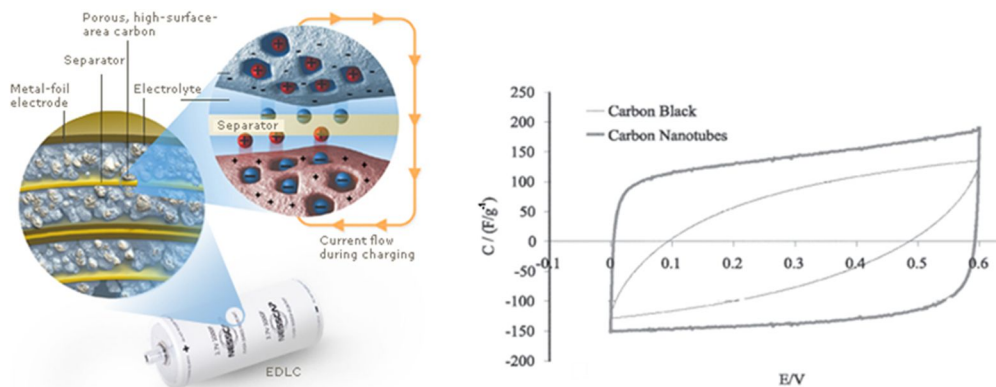


Figure 2: a) Behavior of EDLC b) cyclic voltammetry of EDLC

However, because rGO has poor electrical conductivity, rGO alone as a supercapacitor material lacks the electrochemical performance of the device [10]. Therefore, many researches have been done in incorporating pseudocapacitive materials such as metal oxides in order to create synergistic effects and improve the electrochemical performance [11].

1.1.2 Metal oxide (MO) as electrode material for pseudocapacitor and its pseudocapacitive behavior

By introducing the loading of metal oxides (MO) onto the surface of rGO,

synergistic effects of porosity of rGO and well defined redox mechanism of MO have been known to improve the electrochemical performance of the pseudocapacitor [4]. Since metal oxides have very high theoretical specific capacitance with well-defined redox mechanism, it contributes greatly to the pseudocapacitive behavior of the pseudocapacitor [9]. As seen in Figure 3a [12], when compared to rGO, MO interact with electrolyte ions through electrochemical reaction where redox reactions happen between MO and the ions. Meaning, there must be a change in the oxidation state of the metal oxide as it reacts with the charged electrolyte ions. Thus, giving pseudocapacitive peaks in cyclic voltammetry as seen in Figure 3b [12].

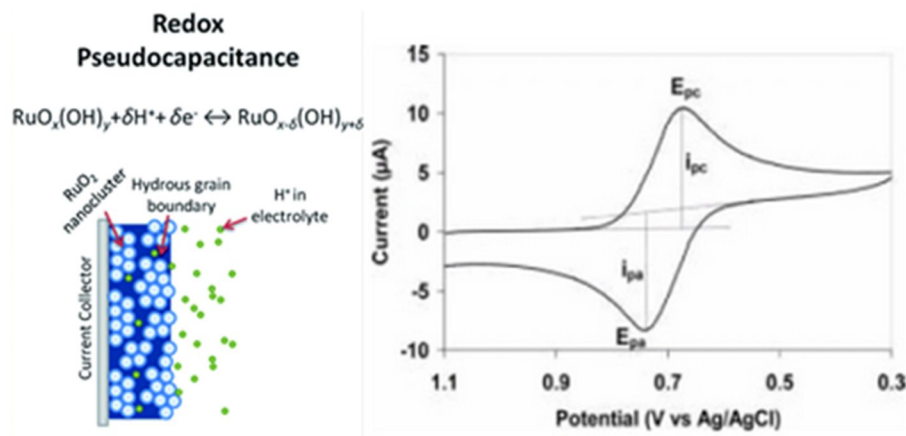


Figure 3: a) Behavior of pseudocapacitor b) cyclic voltammetry of pseudocapacitor

Many metal oxides have been researched on as candidates for electrode materials. Among them, ruthenium oxide (RuO₂) and iridium oxide (IrO₂) show very high electrochemical performance, however these noble metal oxides are very

expensive, thus giving us restraints to using them commercially [4]. Therefore, alternate cheap metal oxides have been researched on such as manganese oxide (MnO_2) [13], ferric oxide (Fe_2O_3) [14], nickel oxide (NiO) [15], and cobalt oxide (Co_3O_4) [16].

We have decided to use Co_3O_4 as our metal oxide material because of its advantages such as having low cost, high redox reactivity, high theoretical specific capacitance ($\sim 3560 \text{ F/g}$), and high reversibility [4]. By incorporating Co_3O_4 into rGO substrate, we were able to fabricate rGO/MO pseudocapacitor

1.1.3 Important factors for performance of pseudocapacitor

It is important to consider different parameters that affect the electrochemical performance of pseudocapacitors. In order to achieve high electrochemical performance, the pseudocapacitor must show high specific capacitance. Specific capacitance can be calculated using the following equation [17]:

$$C_{sp} = \frac{\int I(V)dV}{mv\Delta V} = \left(\frac{\epsilon_r \epsilon_o}{d} \right) \quad (1)$$

Where C_{sp} , I , m , v , and ΔV are specific capacitance, current at charge-discharge, mass of 2 electrodes, scan rate, and potential window respectively. And ϵ_r , ϵ_o , d , A are relative permittivity, permittivity of vacuum, effective thickness of the supercapacitor, and specific surface area of the electrode respectively. The parameters $\int I$, v , and ΔV

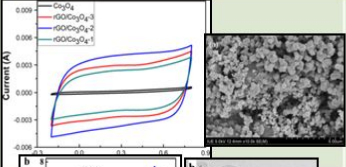
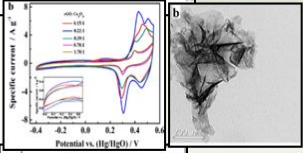
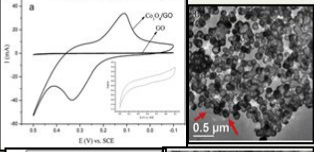
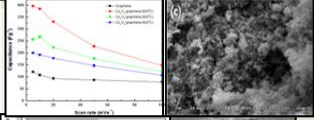
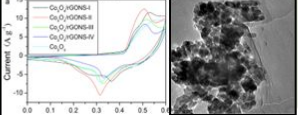
may be obtained from cyclic voltammetry graphs such as the one shown in Figure 3b.

In order to increase the specific capacitance values, the parameters ϵ_r , d , and A are important to consider. These parameters solely consider the nature of the supercapacitor itself. In order to increase ϵ_r , the resistance between the electrode material and the electrolyte should be small. In order to control d , the porosity of the electrode material should be controlled. In order to increase the specific surface area, the electrode material must be very porous [4]. Thus, combining all these factors, we generally want high accumulation of electrolyte ions at the surface of the electrode in order to increase the electrical current value, I .

1.1.4 State-of-the-art (SOA) of rGO/Co₃O₄ pseudocapacitors

Currently, many researches have been done on using rGO and Co₃O₄ electrode materials for pseudocapacitors. Though all of these researches indicate that they have similarly used rGO as the porous substrate material and Co₃O₄ as the metal oxide material in the pseudocapacitor, they each show very different morphologies of the Co₃O₄ nanoparticles and very different specific capacitance values as shown in Table 1:

Table 1: SOA of rGO/Co₃O₄ pseudocapacitors

Composite	Method	Specific capacitance (F/g)	Goal stated/Abstract	Reference
rGO/Co ₃ O ₄ composite	Hydrothermal Synthesis (varying ratio of rGO:Co ₃ O ₄)	263		J Mater Sci 48 (2013) 8463–8470
rGO in Co ₃ O ₄ matrix	Chemical Synthesis (varying ratio of rGO:Co ₃ O ₄)	291		Materials Chemistry and Physics 130 (2011) 672 – 679
Co ₃ O ₄ hollow spheres/rGO composite	Solvothermal synthesis	360		Current Applied Physics 13 (2013) 1796 – 1800
Co ₃ O ₄ /graphene composite	Chemical Synthesis (varying heat treatment)	396		Carbon Letters Vol. 13, No. 2, (2012) 130-132
Co ₃ O ₄ /rGO Nanosheets	Hydrothermal Synthesis (varying ratio of rGO:Co ₃ O ₄)	400		Electrochimica Acta 112 (2013) 120 – 126

These researches use similar methods; either hydrothermal or chemical synthesis. However they show very different electrochemical performance. An effort they have tried to improve the electrochemical performance is by varying the ratio of rGO:Co₃O₄, which is a very common way to improve the performance. An example can be seen in Figure 4a, where we can see that the specific capacitance value increases with the ratio of rGO:Co₃O₄ [17].

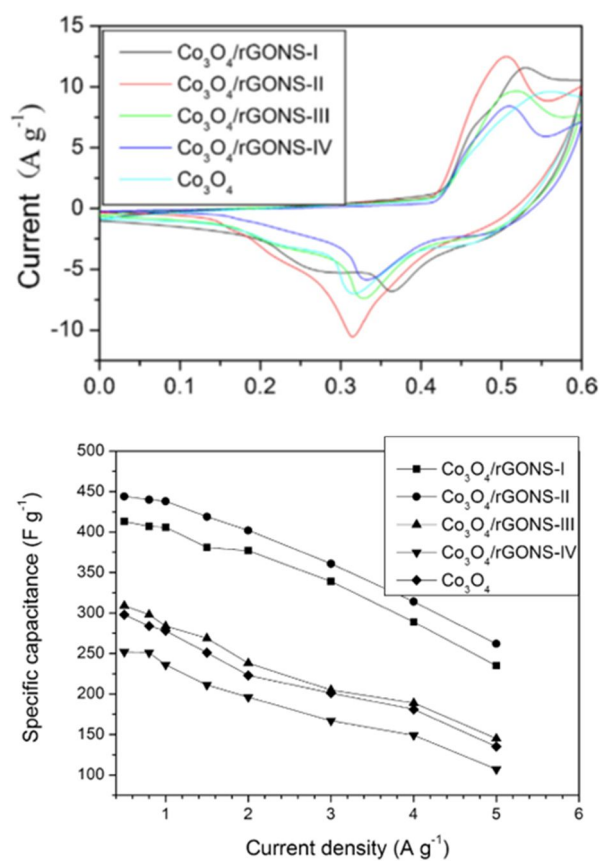


Figure 4: a) Cyclic voltammetry of rGO/ Co_3O_4 pseudocapacitor with varying ratio b)
Specific capacitances of rGO/ Co_3O_4 pseudocapacitor

1.1.5 Limitation of the state-of-the-art of rGO/Co₃O₄ pseudocapacitors

As mentioned in the previous section, the researches of the SOA all similarly use rGO and Co₃O₄ as the electrode material for pseudocapacitor with similar methods. However, they all show very different morphologies and electrochemical performance. These researches only show how to synthesize rGO/MO composite through simple methods just to prove that the pseudocapacitor has a very high specific capacitance and no other research is done on the surface characteristics of the rGO substrate itself. There must be an influence from the graphite precursor itself which gives different graphene oxides with different surface properties and we believe that these properties such as the oxygen functional groups affect the growth of metal oxides on the surface of the rGO substrate.

Therefore, no research was done on verifying which kind of rGO plays the ideal role as a substrate material for the growth of metal oxides in terms of rGO's surface characteristics, chemical properties, and its preparation methods from the graphite precursors. We, therefore, suggest that there must be a difference in electrochemical performance depending on the morphologies of how the metal oxides grew on the surface of the rGO substrate, which we believe is affected by the amount of oxygen functional groups attached.

1.2 The growth of metal oxide on the oxygen functionalized rGO substrate

1.2.1 Interaction of rGO and metal oxides

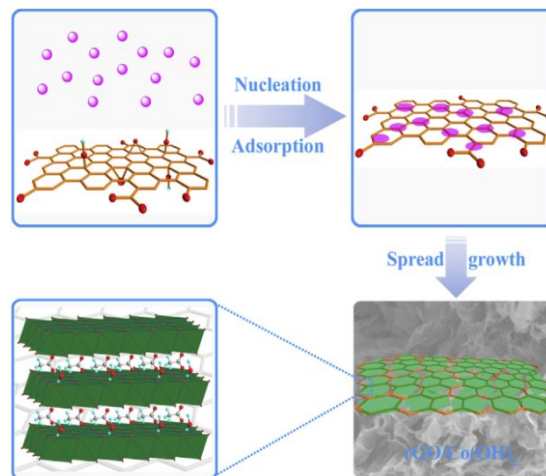


Figure 5: Reaction scheme of reaction between MO and GO

Metal oxides have interfacial interactions with GO by two different types of mechanisms. The first mechanism is the reactive chemisorption on functional groups that bridge the metal centers at the oxygen defect sites. The second mechanism is the Van der Waals interactions between the pristine region of graphene and metal oxides. The reaction scheme can be briefly seen in Figure 5 [4]:

Where the metal oxides first adsorb onto the surface of rGO, then nucleates throughout

the surface, and finally undergoes spread growth to give a rGO/MO composite. Therefore the content of oxygen functional groups attached on the surface of rGO is an important factor to consider.

1.2.2 Growth of metal oxides and its interaction with the functional groups of the rGO

By looking at the SOA of rGO/Co₃O₄ pseudocapacitors, it has come to our attention that there must be an influence of the growth of metal oxides from the surface characteristics of rGO. From looking at the following SOA and Figure 6 [18]:

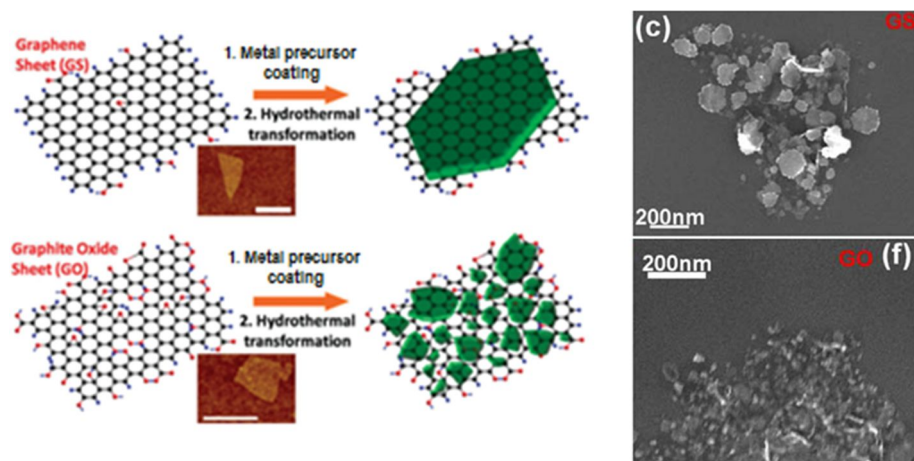


Figure 6: SOA suggesting the difference in growth of MO depending on functional groups attached on GO

We can see that the growth of metal oxides depend on the amount of functional groups attached on the surface of rGO. The graphene sheet with small amount of functional groups show that the metal oxides agglomerate and grow into each other into a big chunk of metal oxide while graphene oxide sheet with large amount of functional groups show that the metal oxides are pinned in between the functional groups and prevent the metal oxides from growing into each other and maintain its crystalline shape as small clusters. From this, we can assume that there must be a difference in the electrochemical performance depending on the available redox reaction sites on the surface of rGO.

1.2.3 Controlling the functional groups of rGO through oxidation

Based on J. Kang's research, the amount of functionalized groups attached on the surface of rGO can be controlled by controlling the oxidation time in the modified Hummer's method. As shown in Figure 7 [19]:

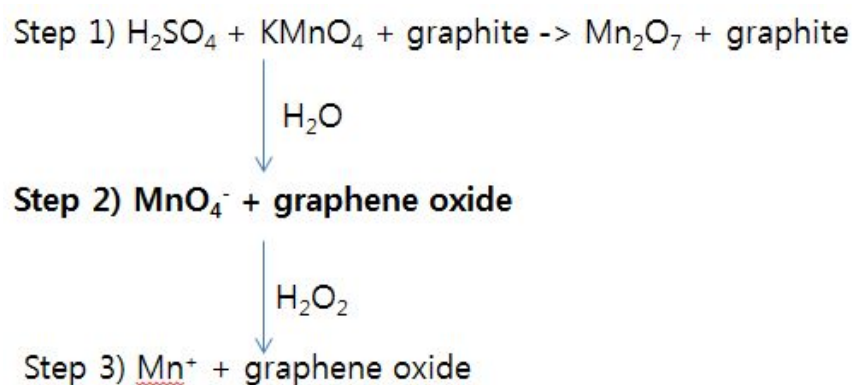


Figure 7: Steps of oxidation of GO

While previous researches focused on step 1, Kang suggested that we must also investigate step 2 and prove that by controlling this step, we may be able to control the amount of functional groups attached on the surface of rGO. Thus, as-proven, by increasing the oxidation time of step 2, we were able to increase the oxygen functional groups and therefore expect the following visualized scheme of the varying GOs in Figure 8:

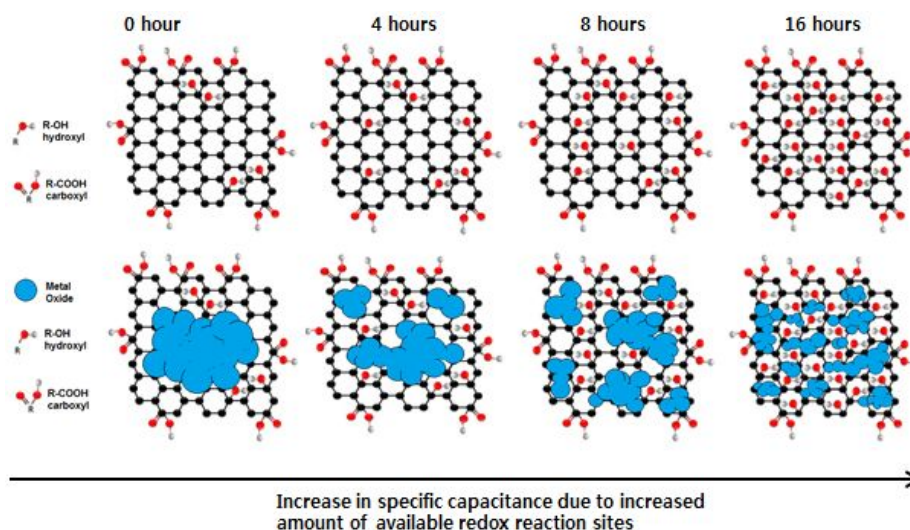


Figure 8: Expectation of the growth of MO on the varied functionalized GO surfaces

1.2.4 Graphite precursors

We will also need to consider the two most commonly used graphite precursors known as small/crumpled graphite (400 mesh) of size $\sim 2\mu\text{m}$ and large/planar graphite (30mesh) of size $\sim 500\mu\text{m}$, which the size difference can be seen in the optical microscopy image in Figure 9a and 9b. After we have distinguished which precursor is a better substrate for growing metal oxides, we will use that graphite precursor to vary the oxidation time and functional groups and continue with the remaining research.

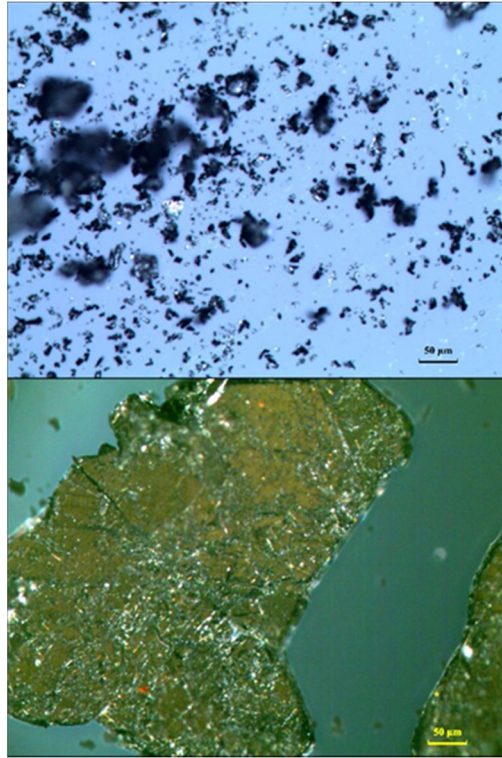


Figure 9: Optical microscopy images of a) small/crumpled GO and b) large/planar GO

1.3 The goal of this research

Again, re-iterating the limitation of the previous researches on the $\text{rGO}/\text{Co}_3\text{O}_4$ pseudocapacitors, the researches typically fabricate a composite and show that it has a high value. No research was done on verifying which kind of rGO plays the ideal role as a substrate for the growth of metal oxides in terms of rGO's surface characteristics, chemical properties, and its preparation methods.

Therefore, we decided to provide a guideline of how to prepare rGO substrate

of different chemical properties and functional groups and its effect of the growth of metal oxides and analyze its relationship between the performance of the pseudocapacitor.

2. Experimental

2.1 Preparation of varied surface properties of rGO

2.1.1 Materials

Small/crumpled graphite precursor (GO (C)), large/planar graphite precursor (GO (P)) purchased from Sigma-Aldrich Korea. KMnO_4 ($\geq 99.0\%$), $(\text{CH}_3\text{COO})_2\text{Co}\cdot 6\text{H}_2\text{O}$ were purchased from Sigma-Aldrich Korea, H_2SO_4 ($\geq 98.0\%$), H_2O_2 , ammonia hydroxide were purchased from Daejung Chemical.

2.1.2 Oxidation of GO(C) and GO(P)

Modified Hummer's method was used for the oxidation of GO. 2.4g of graphite flake was pre-oxidized with 2.0g of potassium persulfate and 2.0g of pentoxide solution in 10ml of concentrated sulfuric acid at $80\text{ }^\circ\text{C}$ for 3days. The expanded graphite was then poured into D.I. water and vacuum filtered and washed again with D.I. water and vacuum dried at room temperature overnight. Step 1: Expanded graphite was then oxidized with 12g KMnO_4 in 92 ml of concentrated sulfuric acid at $35\text{ }^\circ\text{C}$ for 2.5h. Then the mixture was cooled to $0\text{ }^\circ\text{C}$ and 1.0L of D.I. water was poured into the mixture within 30 minutes. Step 2: then 10ml H_2O_2 solution

was put to terminate the oxidation. The obtained GO precipitate was then centrifuged at 10,000 rpm for 15 min and mixed with 1M HCl solution and centrifuged for 3 more times in order to remove the oxidation impurities. Finally, GO was neutralized with D.I. water by centrifugation at 13,000 rpm for 40 min until the PH value became over 5.0 [20,21]

2.1.3 Oxidation of GO(P) at 0h, 4h, 8h, 16h oxidation time

For this part, we incorporated J.H. Kang's oxidation method by increasing the oxidation time of step 2 and left the other parts the same as above. For 0h sample, 10ml H₂O₂ solution was poured after 30 min as indicated above. For 4h, 10ml H₂O₂ solution was poured after 4 hours. For 8h, 10ml H₂O₂ solution was poured after 8 hours. For 16h, 10ml H₂O₂ solution was poured after 16 hours.

A total of 5 different kinds of GO samples were prepared: crumpled GO (oxidation time 0h) will be noted as GO (C), planar GO (oxidation time 0h, 4h, 8h, 16h) will be noted as GO (P-0), GO (P-4), GO (P-8), GO (P-16).

2.2 Preparation of rGO/Co₃O₄ pseudocapacitor

2.2.1 Preparation of rGO/Co₃O₄ composites

The composite was prepared by the method suggested by others [18,22]. 70mg of GO in 70ml D.I. water is dispersed in sonic bath for 2 hours. GO suspension magnetically stirred and 140mg of $(\text{CH}_3\text{COO})_2\text{Co}\cdot 6\text{H}_2\text{O}$ added to the suspension when temperature reaches 50 °C. Mixture then magnetically stirred at 50 °C for 1 hour. Mixture then autoclaved at 180 °C for 12 hours. When mixture has cooled down to room temperature, it was vacuum filtered and washed with D.I. water and ethanol for at least three times each. Obtained sample vacuum dried at room temperature overnight. Finally, the dried sample was calcined at 250 °C for 2hrs at 5 °C/min.

2.2.2 Preparation of rGO/Co₃O₄ electrodes

The obtained rGO/Co₃O₄ sample was mixed with 15 wt% SuperP as conductive material and 5 wt% PTFE as binder material. The obtained flake-like composite was deposited onto 1cm x 10cm large nickel foam by pressure. Full cell was made throughout the whole research. Therefore two electrodes with the composite were made. 6M KOH was used as the electrolyte.

2.3 Characterization of rGO/Co₃O₄ pseudocapacitor

2.3.1 Electrochemical measurement for electrochemical performance of pseudocapacitor

Three electrode system was constructed using Hg/HgO as the reference electrode, Pt as the counter electrode, and the nickel foam and active material as the working electrode. 5M KOH was used as the electrolyte. A battery cycler (WBCS3000, WonATech) was used for cyclic voltammetry and galvanostatic charge/discharge at a fixed potential window of 0.543V at a scan rate of 1, 5 mV/s and 1, 2, 5 Ag⁻¹ for the as-made pseudocapacitors.

2.3.2 Physicochemical analysis of pseudocapacitor

The content of carbon and oxygenated carbon within the GO were investigated by the X-ray photoelectron spectroscopy (XPS; Sigma Probe, Thermo Scientific). The surface characterization of rGO was carried out by powder X-ray diffraction (PXRD; D8 Advance, Bruker) using Ni-filtered Cu K α radiation ($\lambda = 0.154184$ nm). The morphologies of rGO/Co₃O₄ composite was characterized by scanning electron microscopy (SEM; JSM-6700F, JEOL), and analytical transmission electron microscopy (Analytical TEM; Tecnai F20, FEI).

3. Results and Discussion

3.1 Electrochemical and physicochemical analysis of rGO/C₀3O₄(C) and rGO/C₀3O₄ (P)

3.1.1 Electrochemical performance and structural analysis of rGO and C₀3O₄

The cyclic voltammetry (CV) analysis was used for the measurement of solely rGO supercapacitor. As seen in Figure 10:

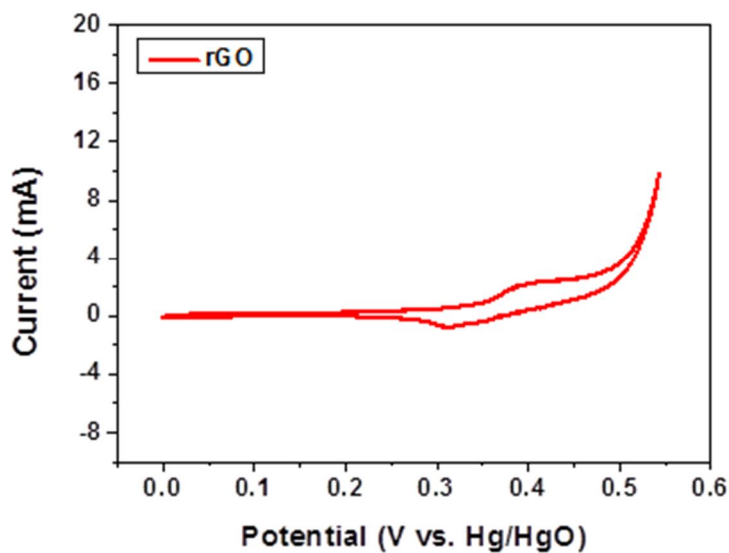


Figure 10: Cyclic voltammetry of rGO

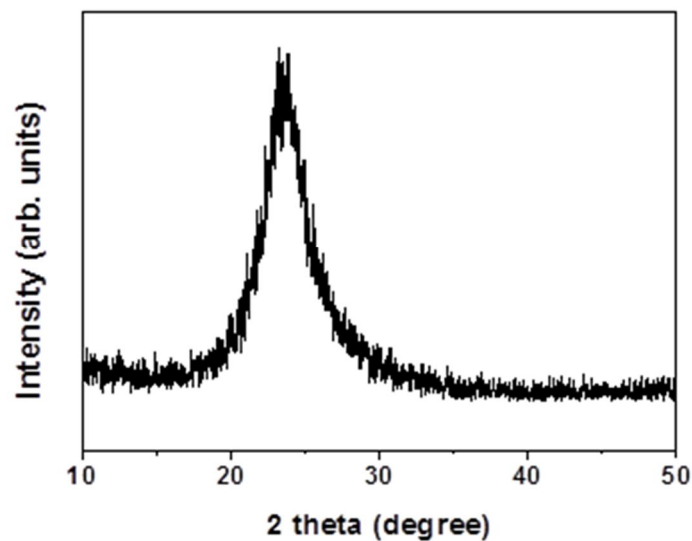


Figure 11: XRD of rGO

We can see that the rGO supercapacitor shows an EDLC behavior as discussed in the introduction section. It has an almost symmetrical rectangular shape with no particular pseudocapacitive peaks suggesting that only electrostatic reactions has happened between the rGO electrodes and the 6M KOH electrolyte ions. And it can be seen from the XRD in Figure 11, confirming that the sample made show its characteristic rGO peak around $\theta = 25^\circ$.

We also fabricated a pseudocapacitor with Co_3O_4 nanoparticles only and the CV curve as seen in Figure 12:

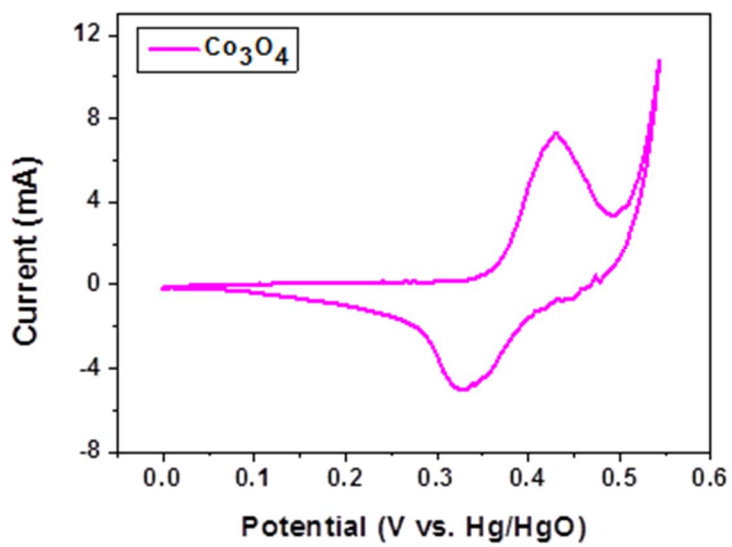


Figure 12: Cyclic voltammetry of Co_3O_4

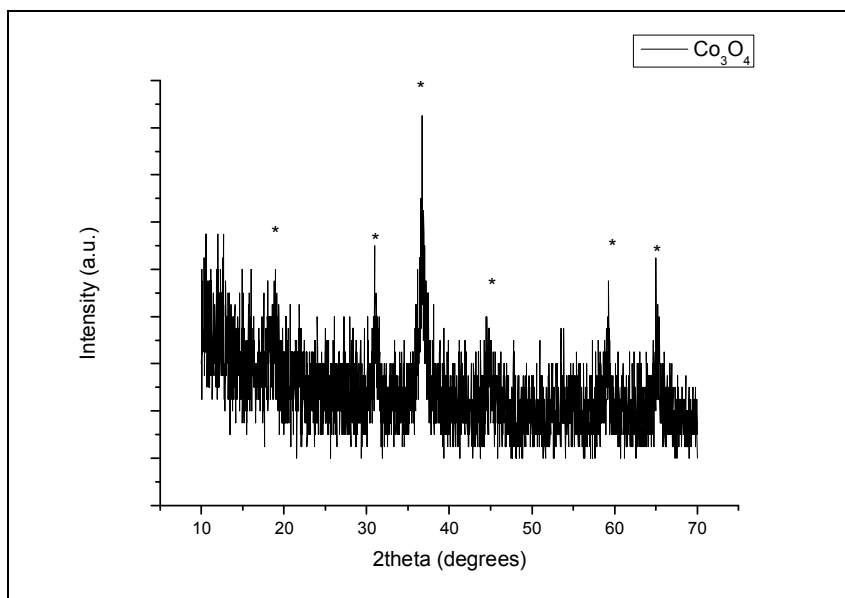


Figure 13: XRD of Co_3O_4

Compared to the rGO supercapacitor, which showed an EDLC behavior, the Co_3O_4 pseudocapacitor show a sharp pseudocapacitive peak at a potential around 0.43V, suggesting that there is definitely an electrochemical reaction happening between the metal oxides and the electrolyte ions. It can also be seen from Figure 13 that the following sample is well fabricated with indicative Co_3O_4 peaks at $\theta = 18.9^\circ, 30.9^\circ, 36.7^\circ, 45.3^\circ, 59.2^\circ, 65.0^\circ$.

3.1.2 Electrochemical performance of $\text{rGO}/\text{Co}_3\text{O}_4(\text{C})$ and $\text{rGO}/\text{Co}_3\text{O}_4(\text{P})$

Figure 14 shows the CV curve of $\text{rGO}/\text{Co}_3\text{O}_4(\text{C})$ and $\text{rGO}/\text{Co}_3\text{O}_4(\text{P})$ composite measured and the specific capacitance values were calculated using equation (1).

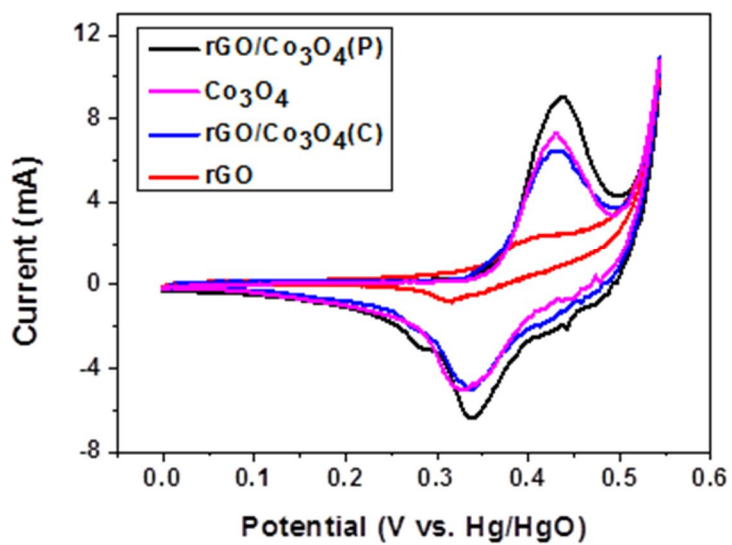


Figure 14: Cyclic voltammetry of rGO/Co₃O₄(P), rGO/Co₃O₄(C), Co₃O₄, and rGO at 5 mV/s

Table 2: Calculated pecific capacitance values of rGO, Co₃O₄, rGO/Co₃O₄(C), rGO/Co₃O₄(P) at 1 A/g

Samples	Specific capacitance (F/g)
rGO	154.8
Co ₃ O ₄	176.6
rGO/Co ₃ O ₄ (C)	178.5
rGO/Co ₃ O ₄ (P)	207.2

As seen in Figure 14, we can see that more pseudocapacitive peak is shown in the rGO/Co₃O₄(P) while the peaks are merely shown in rGO/Co₃O₄(C). Table 2 shows the calculated specific capacitance of rGO supercapacitor, Co₃O₄, rGO/Co₃O₄(C), and rGO/Co₃O₄(P) pseudocapacitors at 1 Ag⁻¹. From this table, we can see that the rGO/Co₃O₄(P) pseudocapacitor show highest specific capacitance compared to the rGO/Co₃O₄(C), suggesting that rGO(P) is a more suitable substrate for growing well dispersed Co₃O₄ nanoparticles.

Before going into details of analyzing why the samples show different electrochemical performances, an XRD analysis of the composites confirm that the Co₃O₄ nanoparticles were well fabricated in the rGO composites as shown in Figure 15.

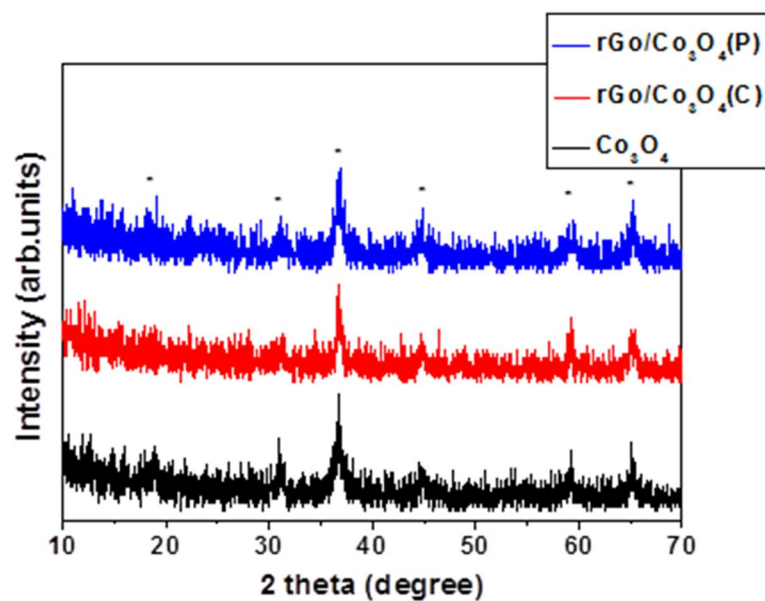


Figure 15: XRD of Co_3O_4 , $\text{rGO}/\text{Co}_3\text{O}_4(\text{P})$, $\text{rGO}/\text{Co}_3\text{O}_4(\text{C})$

3.1.3 Physicochemical analysis of GO(C) and GO(P)

The XPS data in Figure 16a and b show the deconvoluted C1s peak of GO(C) and GO(P). From this figure, we can see that the C-C and C-OH peaks are very similar to each other suggesting that both GO(C) and GO(P) have similar amount of functional groups.

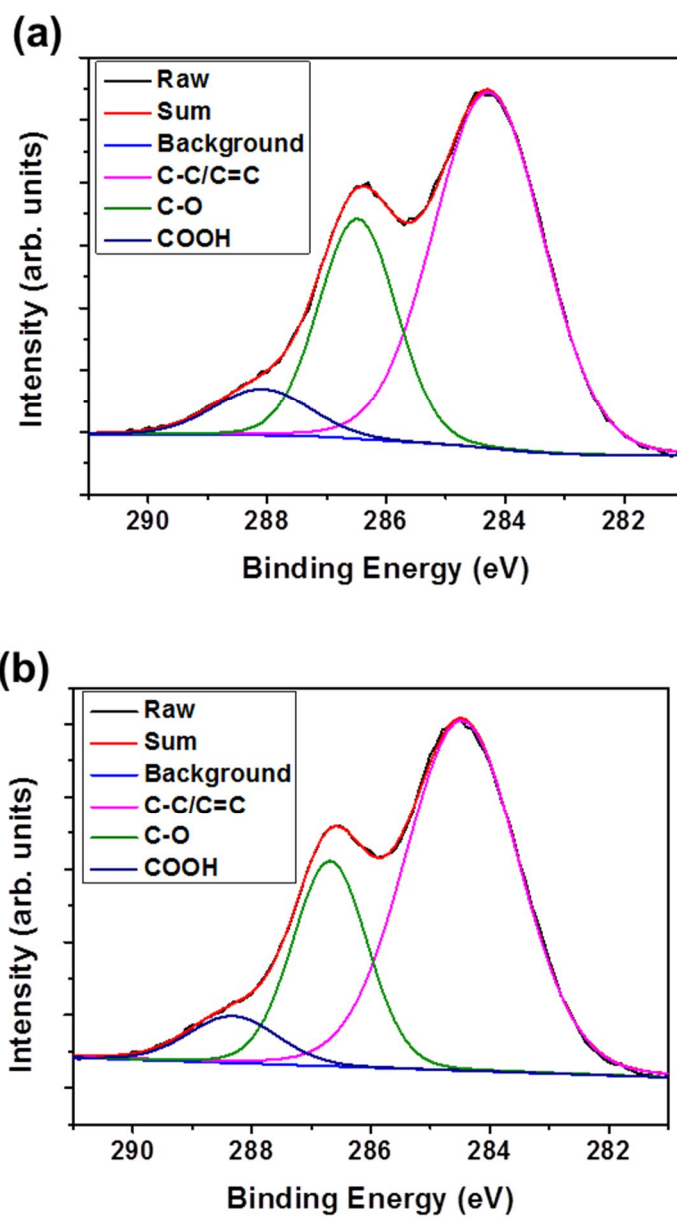


Figure 16: Deconvoluted C1s peak of XPS data of a) GO(P) and b) GO(C)

The percentages of oxygenated carbon was calculated from the XPS data of GO(P) and GO(C) and is summarized in Table 3:

Table 3: Amount of oxygenated carbon calculated from the XPS data of GO(P) and GO(C)

Samples	C=C (%)	C-O (%)	O-C=O (%)
GO(P)	64.4	28.3	7.3
GO(C)	67.1	25.9	7.0

From Table 3, we can see that GO(C) and GO(P) have very similar amount of functional groups, therefore we want to emphasize that the amount of functional groups is not a controlling parameter of this part of the research. The growth of metal oxides was not affected by the number of functional groups.

We also took SEM and TEM images in order to analyze the morphologies of how the Co_3O_4 nanoparticles were grown on the surface of rGO(P) and rGO(C). As seen in Figure 17a and b, we can clearly see the difference between the two composites. For rGO/ Co_3O_4 (P), the Co_3O_4 nanoparticles are well dispersed between the sheets and the MO particles are well packed amongst each other while for rGO/ Co_3O_4 (C), the growth of MO particles itself cannot be clearly seen. Rather, the particles are only grown on some parts or not grown at all. From this we can conclude that rGO(P) is a more suitable substrate for growing metal oxide nanoparticles.

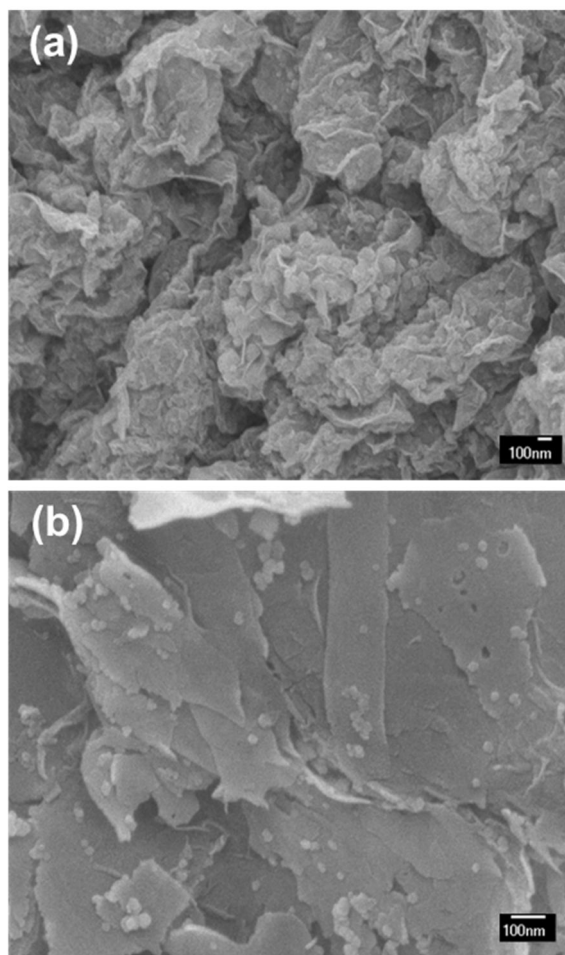


Figure 17: SEM images of a) rGO/Co₃O₄(P) and b) rGO/Co₃O₄(C)

3.2 Electrochemical and physicochemical analysis of rGO/C₀3O₄(P-0), rGO/C₀3O₄(P-4), rGO/C₀3O₄(P-8), rGO/C₀3O₄(P-16)

3.2.1 Physicochemical analysis of GO(P-0), GO(P-4), GO(P-8), GO(P-16) and rGO/C₀3O₄(P-0), rGO/C₀3O₄(P-4), rGO/C₀3O₄(P-8), rGO/C₀3O₄(P-16)

The XPS data in Figure 18 show the deconvoluted C1s peak of GO treated at 4 different oxidation times – 0h, 4h, 8h, 16h. From this figure, we can see that the C-C and C-OH peaks differ between GO treated at 0h and 16h. It can be seen that the area of the C-O peaks increase as the oxidation time increases indicating an increase in oxygen functional groups. This was thus shown in a bar graph shown in Figure 20. From this Figure, we can see that as the C-O bond increases, the C-C bond decreases with, which is again shown in Table 4.

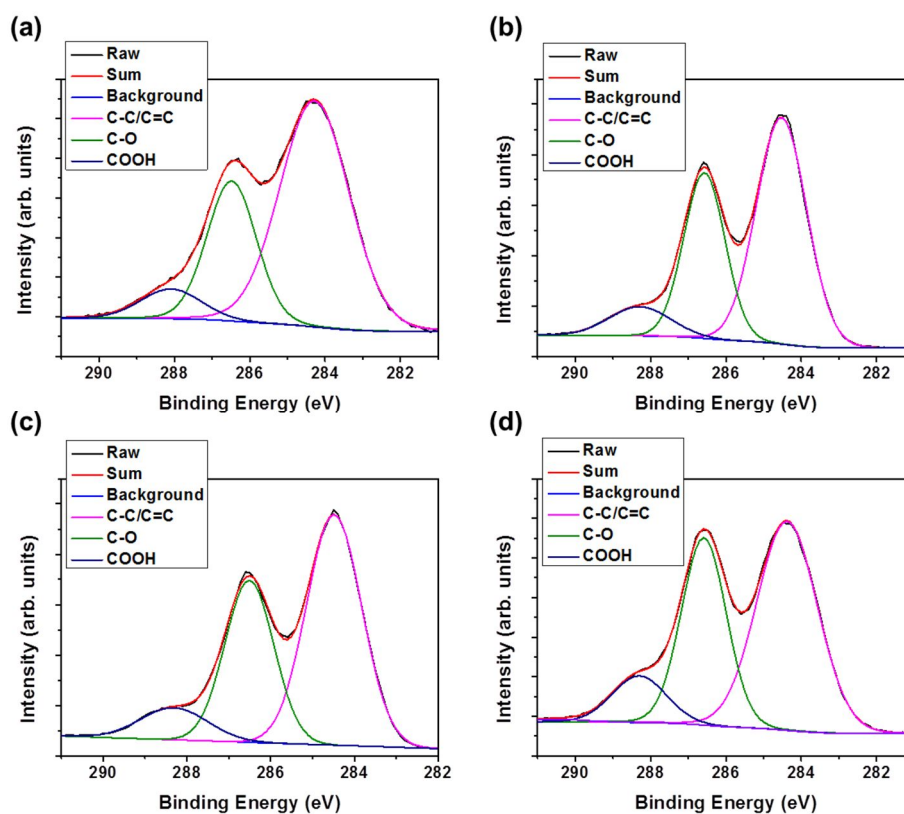


Figure 18: Deconvoluted C1s peak of XPS data of (a) GO(P-0) and (b) GO(P-4) (c) GO(P-8) (d) GO(P-16).

Table 4: Percentages of oxygenated carbon calculated from the XPS data of GO(P-0), GO(P-4), GO(P-8), GO(P-16)

Samples	C=C (%)	C-O (%)	O-C=O (%)
GO(P-0)	64.4	28.3	7.3
GO(P-4)	56.9	34.2	8.9
GO(P-8)	55.8	34.8	9.4
GO(P-16)	53.7	35.7	10.6

From Table 4, it can be seen that the percentage of oxygenated carbon increases with oxidation time of GO. This is because the contact time between MnO_4^- and GO increases with the oxidation time. The more GO is exposed to MnO_4^- , the more functional groups are attached to the surface of GO.

Now that we have confirmed that the functional groups of GO increase with the oxidation time, we utilized the four different types of GO into fabricating $\text{rGO/Co}_3\text{O}_4$ – 0h, 4h, 8h, 16h. We first were able to confirm from the XRD that all four composites were well fabricated with Co_3O_4 well incorporated into the composite as shown in Figure 19 with the indicative Co_3O_4 peaks.

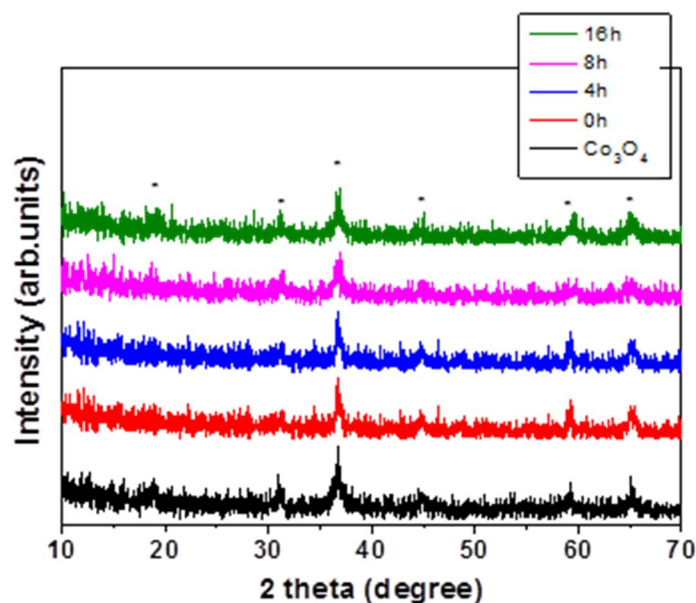


Figure 19: XRD of Co_3O_4 , $\text{rGO}/\text{Co}_3\text{O}_4(\text{P-0})$, $\text{rGO}/\text{Co}_3\text{O}_4(\text{P-4})$, $\text{rGO}/\text{Co}_3\text{O}_4(\text{P-8})$, $\text{rGO}/\text{Co}_3\text{O}_4(\text{P-16})$

After confirming that the composites were all well fabricated with indicative Co_3O_4 nanoparticles, we took SEM and TEM images of the four different types of composites in order to analyze the morphology of the composites. As seen in Figure 20a, b, c, d, we can see that for $\text{rGO}/\text{Co}_3\text{O}_4(\text{P-0})$ and $\text{rGO}/\text{Co}_3\text{O}_4(\text{P-4})$, the Co_3O_4 nanoparticles are only grown on some parts of the GO surface. Some parts don't have any Co_3O_4 nanoparticles grown at all. For $\text{rGO}/\text{Co}_3\text{O}_4(\text{P-8})$ and $\text{rGO}/\text{Co}_3\text{O}_4(\text{P-16})$, we can see that the Co_3O_4 particles are actually very well dispersed onto the surface of GO.

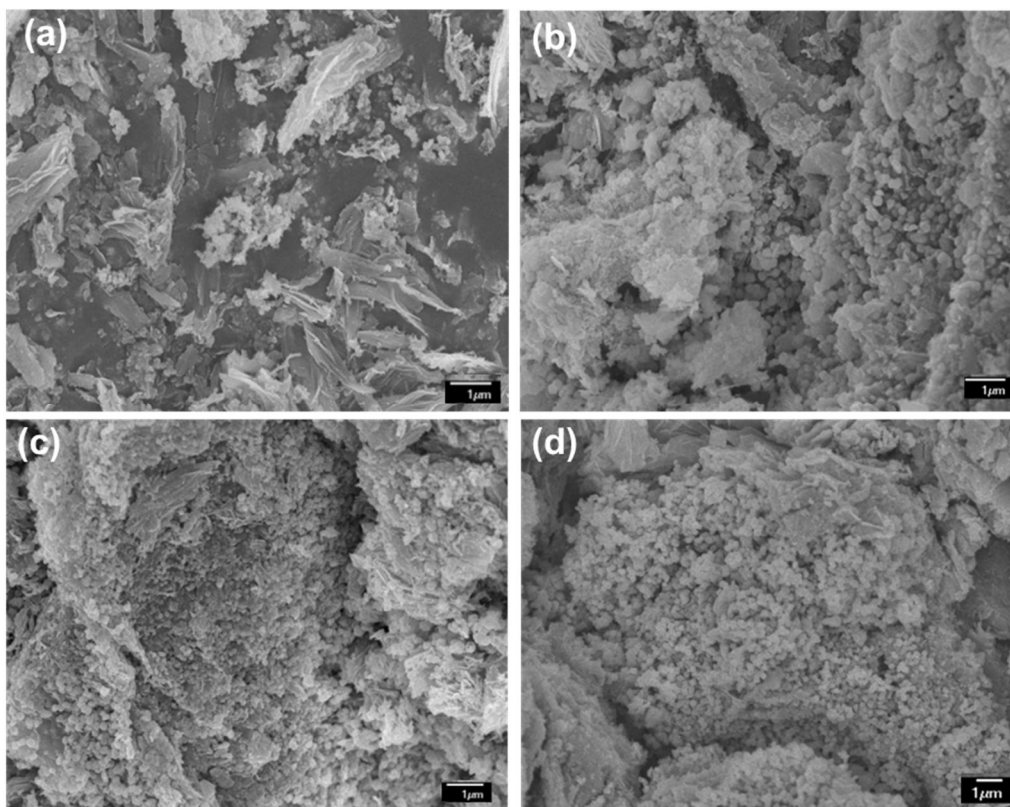


Figure 20: SEM images of (a) rGO/Co₃O₄(P-0) (b) rGO/Co₃O₄(P-4) (c) rGO/Co₃O₄(P-8) (d) rGO/Co₃O₄(P-16).

In order to look into the morphology into more detail in regarding the sizes of the Co₃O₄ nanoparticles, we took TEM images of the four composites. As shown in Figure 21a, b, c, d, we can see that for rGO/Co₃O₄(P-0) and rGO/Co₃O₄(P-4), the Co₃O₄ nanoparticles are grown into each other into very big sized nanoparticles while for rGO/Co₃O₄(P-8) and rGO/Co₃O₄(P-16), the Co₃O₄ nanoparticles are well dispersed onto the sheets of graphene oxide showing that the MO particles are well pinned between the functional groups and therefore not growing into each other.

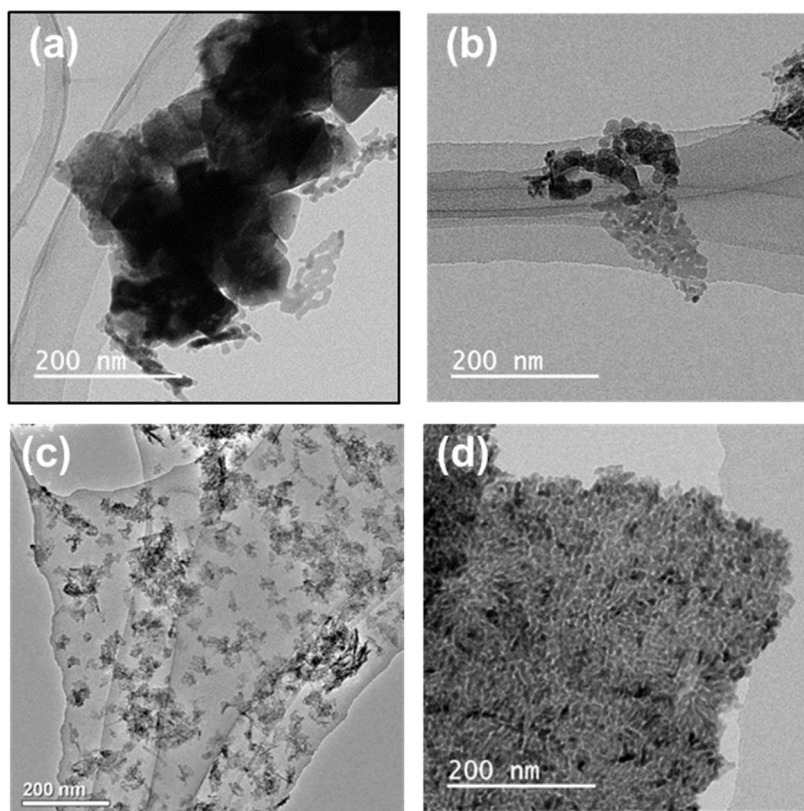


Figure 21: TEM images of (a) rGO/Co₃O₄(P-0) (b) rGO/Co₃O₄(P-4) (c) rGO/Co₃O₄(P-8) (d) rGO/Co₃O₄(P-16).

The particle sizes were approximated from the TEM images and were put into Table 5:

Table 5: Particle sizes and surface coverage of Co_3O_4 grown on $\text{rGO}/\text{Co}_3\text{O}_4(\text{P-0})$, $\text{rGO}/\text{Co}_3\text{O}_4(\text{P-4})$, $\text{rGO}/\text{Co}_3\text{O}_4(\text{P-8})$, $\text{rGO}/\text{Co}_3\text{O}_4(\text{P-16})$

Samples	$\text{rGO}/\text{Co}_3\text{O}_4$ (P-0)	$\text{rGO}/\text{Co}_3\text{O}_4$ (P- 4)	$\text{rGO}/\text{Co}_3\text{O}_4$ (P- 8)	$\text{rGO}/\text{Co}_3\text{O}_4$ (P- 16)
Size (nm)	54.3±18.4	26.3±6.3	9.4±1.9	5.9±1.5
Surface coverage (%)	17.6	30.3	66.2	73.4

From Table 5, we can see that the Co_3O_4 particle size decreases while surface coverage increases with the increasing oxidation time and thus with the increasing functional groups because of the reasons explained above. The smaller sizes of Co_3O_4 particles help them to be more dispersed well on the rGO's surface, thus, providing more available redox reaction sites for the pseudocapacitor..

EDS measurements were also taken along with the TEM images in order to confirm that the Co_3O_4 nanoparticles were well grown on the surfaces of rGO, which is shown in Figure 22. $\text{rGO}/\text{Co}_3\text{O}_4(\text{P-16})$ sample was taken into account owing to its abundancy of Co_3O_4 nanoparticles dispersed onto the surface of rGO. As seen in Figure 22, according to the elemental analysis, cobalt particles can be much more distinctly seen than the carbon detected, indicating that the Co_3O_4 nanoparticles are well grown and dispersed throughout the surface of rGO.

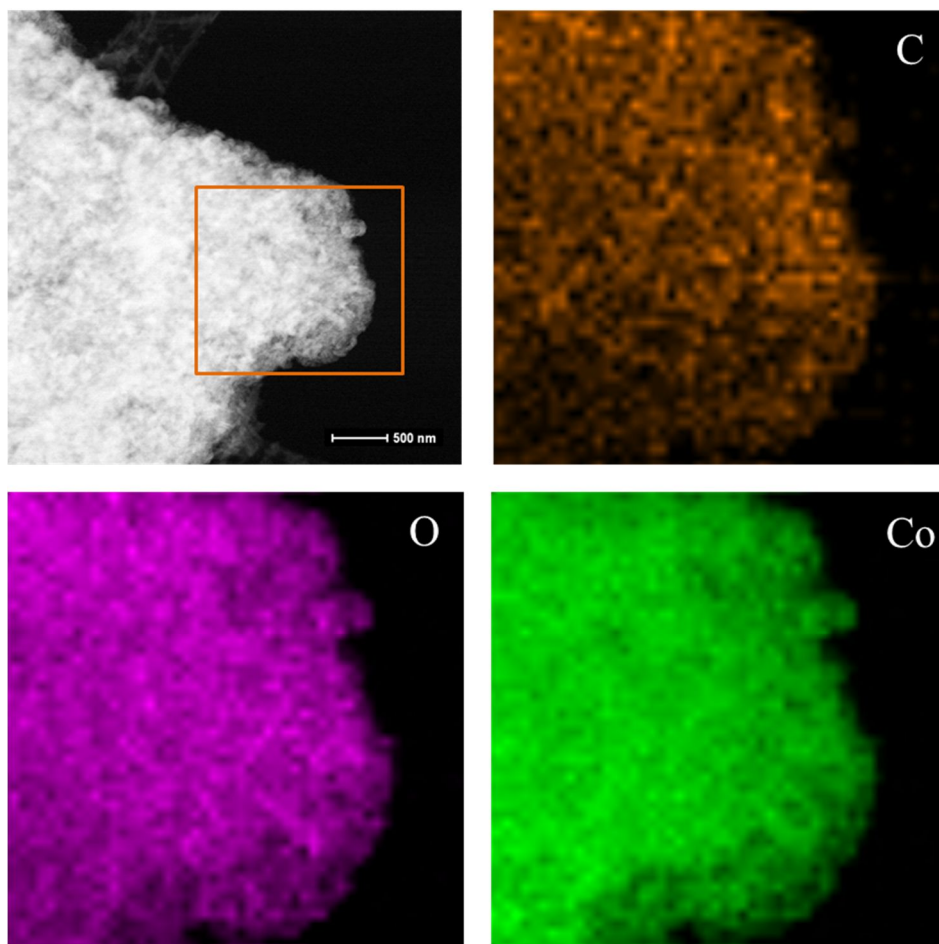
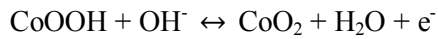
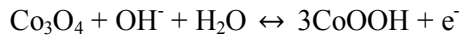


Figure 22: EDS measurements of rGO/Co₃O₄(P-16)

3.2.2 Electrochemical analysis of rGO/Co₃O₄(P-0), rGO/Co₃O₄(P-4), rGO/Co₃O₄(P-8), rGO/Co₃O₄(P-16)

CV measurement was done on the four different composites as shown in

Figure 23. All 4 curves show strong redox peaks indicating faradaic reaction between the Co_3O_4 nanoparticles and the KOH electrolyte ions. Such redox peaks result from the conversion of cobalt oxidation states shown in the following electrochemical reactions:



where two redox couples, $\text{Co}_3\text{O}_4/\text{CoOOH}$ and $\text{CoOOH}/\text{CoO}_2$ are involved. As the area under the curve increase with the oxidation time, the corresponding peaks increase also. This is because, as discussed just before, $\text{rGO}/\text{Co}_3\text{O}_4(\text{P-16})$ has much more Co_3O_4 nanoparticles to faradaically react with the electrolyte ions increasing the accumulation of charges at the certain voltage. This, thus, confirms that our expectation was correct about the availability of redox reaction sites and its relation to the behavior of a pseudocapacitor. Equation 1 was again used to calculate the specific capacitances of the four composites, which are shown in Table 6.

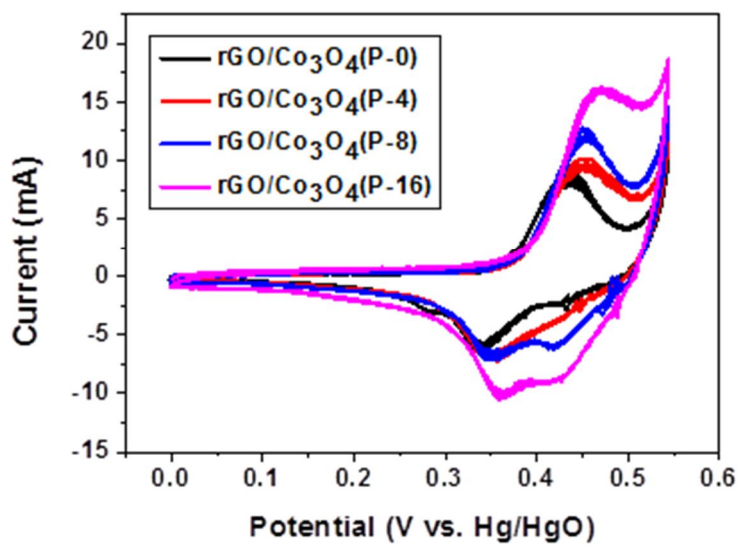


Figure 23: Cyclic voltammograms of rGO/Co₃O₄(P-0), rGO/Co₃O₄(P-4), rGO/Co₃O₄(P-8), rGO/Co₃O₄(P-16) at 5 mV/s

Table 6: Calculated specific capacitance values of rGO/Co₃O₄(P-0), rGO/Co₃O₄(P-4), rGO/Co₃O₄(P-8), rGO/Co₃O₄(P-16) at 1 Ag⁻¹

Samples	Specific capacitance (F/g)
rGO/Co ₃ O ₄ (P-0)	207.2
rGO/Co ₃ O ₄ (P-4)	244.9
rGO/Co ₃ O ₄ (P-8)	320.5
rGO/Co ₃ O ₄ (P-16)	411.5

As shown in Table 6, we can see that the specific capacitance increases with the oxidation time and thus with the functional groups attached on GO due to the reasons that were stated above.

3.3 Correlation graphs

From the final results, we were able to come up with two correlation graphs. The first, shown in Figure 24a, relate the specific capacitance values between rGO, Co_3O_4 , rGO/ $\text{Co}_3\text{O}_4(\text{C})$, and rGO/ $\text{Co}_3\text{O}_4(\text{P})$. From this graph, we can conclude that the specific capacitance is low for the rGO and Co_3O_4 pseudocapacitors alone while it increases a little for the rGO/ $\text{Co}_3\text{O}_4(\text{C})$. However, the rGO/ $\text{Co}_3\text{O}_4(\text{P})$ has the highest specific capacitance because it is a more suitable substrate for growing MO particles.

From Figure 25b, we were able to conclude that the specific capacitance value increases with the oxidation time and thus with the functional groups attached on the surface of GO because of the availability of redox reaction sites in the one with many functional groups.

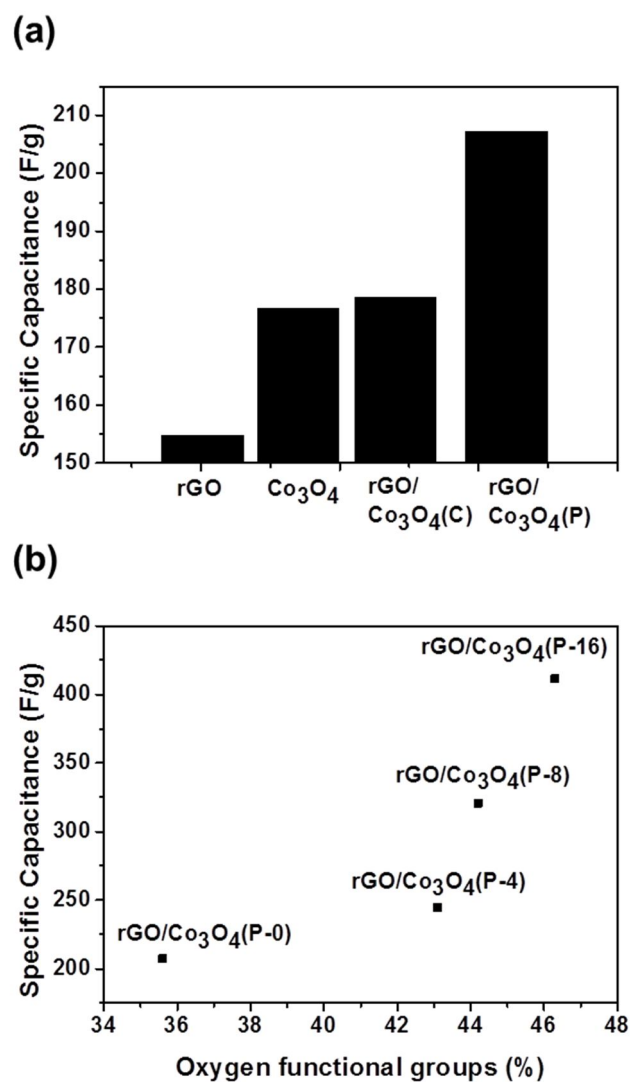


Figure 24: Correlation graphs of (a) specific capacitance vs. samples rGO/Co₃O₄(P-0), rGO/Co₃O₄(P-4), rGO/Co₃O₄(P-8), rGO/Co₃O₄(P-16) at 1 A/g. (b) specific capacitance vs. oxygen functional groups for rGO/Co₃O₄(P-0), rGO/Co₃O₄(P-4), rGO/Co₃O₄(P-8), rGO/Co₃O₄(P-16) at 1 A/g.

4. Conclusion

From this research, we were able to re-visit the oxidation of GO by controlling the oxidation time of GO and investigate its effect in the growth of metal oxides and prove that there is a difference in electrochemical performance for differently oxidized GO with different amount of functional groups attached.

We can first conclude, that rGO and Co_3O_4 pseudocapacitor alone shows poor electrochemical performance. And though they had similar amount of functional groups, rGO/ Co_3O_4 (P) showed better electrochemical performance. Co_3O_4 particles were well dispersed onto the surface of planar rGO, confirming that rGO(P) is more suitable for growing metal oxide nanoparticles.

Secondly, we were able to conclude that rGO/ Co_3O_4 composite fabricated from GO treated for 16h showed the highest electrochemical performance. The more oxygen functional groups, the more nucleation sites for metal oxides to grow in smaller sizes and disperse well, thus, leading to higher specific capacitance value.

5. Reference

- [1] Lightcap, I. V.; Kosel, T. H.; Kamat, P. V. *Nano Letters* **2010**, *10*, 577.
- [2] Ma, L.-P.; Wu, Z.-S.; Li, J.; Wu, E.-D.; Ren, W.-C.; Cheng, H.-M. *International Journal of Hydrogen Energy* **2009**, *34*, 2329.
- [3] Wang, X.; Zhi, L.; Tsao, N.; Tomović, Ž.; Li, J.; Müllen, K. *Angewandte Chemie International Edition* **2008**, *47*, 2990.
- [4] Wu, Z.-S.; Zhou, G.; Yin, L.-C.; Ren, W.; Li, F.; Cheng, H.-M. *Nano Energy* **2012**, *1*, 107.
- [5] <http://www.bccresearch.com/market-research/advanced-materials/graphene>; BCC Research.
- [6] Geim, A. K.; Novoselov, K. S. *Nat Mater* **2007**, *6*, 183.
- [7] Pumera, M. *Chemical Society Reviews* **2010**, *39*, 4146.
- [8] Béguin, F. *Journal of the Brazilian Chemical Society* **2006**, *17*, 1083.
- [9] M. S. Halper, J. C. E. *Supercapacitors: A Brief Overview*, MITRE Report, 2006.
- [10] Lv, W.; Tang, D.-M.; He, Y.-B.; You, C.-H.; Shi, Z.-Q.; Chen, X.-C.; Chen, C.-M.; Hou, P.-X.; Liu, C.; Yang, Q.-H. *ACS Nano* **2009**, *3*, 3730.
- [11] Yang, X.; Zhang, L.; Zhang, F.; Zhang, T.; Huang, Y.; Chen, Y. *Carbon* **2014**, *72*, 381.
- [12] Li, J.; Yang, M.; Wei, J.; Zhou, Z. *Nanoscale* **2012**, *4*, 4498.
- [13] Hsieh, C.-T.; Lin, C.-Y.; Lin, J.-Y. *Electrochimica Acta* **2011**, *56*, 8861.
- [14] Mishra, A. K.; Ramaprabhu, S. *The Journal of Physical Chemistry C* **2011**, *115*, 14006.
- [15] Kottegoda, I. R. M.; Idris, N. H.; Lu, L.; Wang, J.-Z.; Liu, H.-K. *Electrochimica Acta* **2011**, *56*, 5815.
- [16] Yang, S.; Feng, X.; Ivanovici, S.; Müllen, K. *Angewandte Chemie International Edition* **2010**, *49*, 8408.
- [17] Song, Z.; Zhang, Y.; Liu, W.; Zhang, S.; Liu, G.; Chen, H.; Qiu, J. *Electrochimica Acta* **2013**, *112*, 120.

- [18] Wang, H.; Robinson, J. T.; Diankov, G.; Dai, H. *Journal of the American Chemical Society* **2010**, *132*, 3270.
- [19] Kang, J. H. 2015.
- [20] Yang, S. J.; Kim, T.; Jung, H.; Park, C. R. *Carbon* **2013**, *53*, 73.
- [21] Bianco, A.; Cheng, H.-M.; Enoki, T.; Gogotsi, Y.; Hurt, R. H.; Koratkar, N.; Kyotani, T.; Monthieux, M.; Park, C. R.; Tascon, J. M. D.; Zhang, J. *Carbon* **2013**, *65*, 1.
- [22] Liu, G.-J.; Fan, L.-Q.; Yu, F.-D.; Wu, J.-H.; Liu, L.; Qiu, Z.-Y.; Liu, Q. *J Mater Sci* **2013**, *48*, 8463.

국문 초록

이 논문은 환원된 그래핀 옥사이드의 표면특성이 유사커패시터의 성능에 미치는 영향에 대해 연구한 것이다. 환원된 그래핀 옥사이드의 여러 가지 뛰어난 성능으로 인해 이를 적용하려는 다양한 연구가 진행되고 있다. 그 중에서도 금속산화물을 환원된 그래핀 옥사이드의 표면에 성장시켜 유사커패시터의 전극 물질로 사용하는 연구가 진행되고 있다. 금속산화물을 다기공성의 환원된 그래핀 옥사이드에 성장시킬 경우, pseudocapacitive한 특성과 specific capacitance가 향상되는데, 이는 금속산화물의 잘 알려진 redox mechanism과 환원된 그래핀 옥사이드의 높은 전기전도도 덕분이다. 그러나 기존의 연구들은 금속산화물의 성장이 환원된 그래핀 옥사이드의 표면 특성의 개질에 따라 어떠한 차이를 보이는지에 대한 답을 제시하지 않고 성능을 높이는 데에 집중하였다. 따라서 본 연구에서는 그래핀 옥사이드의 표면에 존재 하는 작용기의 양을 조절하여 금속산화물의 성장에 어떠한 영향을 끼치는지 확인하였다. 그래핀 옥사이드에 존재하는 작용기의 양은 산화시간을 조절하여 변화시켰고, 이를 XPS를 통해 확인하였다. 이에 따라 성장한

금속산화물의 크기와 분산도는 SEM과 TEM 측정을 통해 확인하였으며, 제작한 환원된 그래핀 옥사이드/금속산화물 복합체의 specific capacitance는 cyclic voltammetry를 통해 측정하였다. 그 결과 그래핀 옥사이드에 존재하는 작용기의 양이 증가할수록 금속산화물의 크기는 감소하며 분산도는 증가하였고 이에 따라 specific capacitance도 증가하였다.

본 연구는 그래핀 옥사이드의 표면 특성에 따른 금속산화물의 성장 및 분산도를 다양한 분석방법을 통해 다각도로 분석하고, 유사커패시터로서의 전기화학적 성능을 확인하였고, 앞으로 그래핀을 이용한 유사커패시터의 제작에 가이드라인이 될 것이라고 생각한다.

주요어 : 환원된 그래핀 옥사이드, 산화작용기, 금속산화물, 전기화학, 유사캐패시터.

학 번 : 2012-23927